Appendix

Distinct modes of recruitment of the CCR4-NOT complex by *Drosophila* and vertebrate Nanos

Tobias Raisch, Dipankar Bhandari, Kevin Sabath, Sigrun Helms, Eugene Valkov, Oliver Weichenrieder and Elisa Izaurralde

Contents

Appendix Supplementary Materials and Methods

DNA constructs

Luciferase reporters and plasmids for the expression of GFP- or HA-tagged subunits of the CCR4-NOT and PAN2-PAN3 deadenylase complexes, decapping factors, DCP2 catalytic mutant (E361Q) and GW182 were previously described (Behm-Ansmant *et al*, 2006; Tritschler *et al*, 2008; Haas *et al*, 2010). An F-luc-*hb* reporter was generated by inserting the *hunchback* 3' UTR (CG9786) into the NheI and XhoI restriction sites of plasmid pAc5.1-F-Luc (Behm-Ansmant *et al*, 2006). Plasmids for the expression of GFP and λN-HA tagged *Dm* Nanos (Uniprot A0A0B4KGY5-1) were obtained by inserting the cDNA corresponding to the Nanos ORF into the EcoRI and XhoI sites of the pAC5.1-EGFP and pAC5.1-λNHA vectors (Behm-Ansmant *et al*, 2006). Nanos fragments were amplified by PCR using the full-length Nanos template and inserted into the same vectors. Deletion constructs were made by site-directed mutagenesis using appropriate primers. To generate the chimeric NIM-ZnF construct, we inserted a cDNA corresponding to the *Hs* Nanos2 NIM motif (codon-optimized for expression in *Dm*) followed by a Gly-Ser-Ser-Gly linker between the GST and *Dm* Nanos ZnF sequences of the pAC5.1-λNHA-GST-ZnF plasmid.

For the expression of recombinant proteins in *E. coli*, synthetic cDNAs (codon-optimized for expression in *E. coli*) corresponding to *Dm* Nanos fragments were inserted into the XhoI and BamHI restriction sites of the pnEA-pG plasmid (Diebold *et al*, 2011), generating protein fusions containing N-terminal GST tags cleavable by the HRV3C protease. The NED and NED-ΔNBR constructs contain a C-terminal GB1 tag (Chen and Patel, 2004) fused to the Nanos sequences by a Gly-Ser-Ser-Gly linker.

Plasmids for the expression of the *Hs* NOT1 SHD and the NOT2 and NOT3 C-terminal regions have been previously described (Boland *et al*, 2013; Bhandari *et al*, 2014). Human NOT2 and NOT3 were expressed from a bicistronic plasmid based on the pnEA vector

(Diebold *et al*, 2011) and contained HRV3C-cleavable MBP and 6xHis tags, respectively. The DNA constructs used in this study are listed in Appendix Table S1.

mRNA half-live

For the measurement of mRNA half-lives, transfected cells were treated with actinomycin D (5µg/ml final concentration) 3 days after transfection, and harvested at the time points indicated. RNA samples were analyzed by Northern blot. mRNA reporter levels were normalized to the levels of *rp49* mRNA and were plotted against time. The mRNA half-lives ($t_{1/2}$) ± standard deviations were calculated from the decay curves (not shown) obtained from three independent experiments and are indicated below the panels.

Protein expression and purification

All proteins for crystallization and *in vitro* pulldown assays were expressed in *E. coli* BL21 (DE3) Star cells (Invitrogen) in ZY medium at 20 °C overnight. *Dm* Nanos constructs were expressed with N-terminal GST tags. The NED constructs carried, in addition a C-terminal noncleavable GB1 tag. The cells were resuspended and lysed in binding buffer containing 50 mM HEPES (pH 7.5), 300 mM NaCl and 2 mM dithiothreitol (DTT) supplemented with protease inhibitors, lysozyme and DNaseI. The proteins were isolated from the crude lysate using Protino glutathione agarose 4B beads (Macherey Nagel) and eluted in binding buffer containing 25 mM glutathione. For GST pulldown assays, the proteins were further purified by anion exchange chromatography using a HiTrap Q column (GE Healthcare) followed by size-exclusion chromatography using a Superdex 200 column (GE Healthcare) in a buffer containing 10 mM HEPES (pH 7.5), 200 mM NaCl and 2 mM DTT. For crystallization, the GST tag was cleaved after elution from the glutathione beads by incubating overnight with

recombinant HRV3C protease. The protein was separated from the tag by gel filtration on a Superdex 75 26/60 column (GE Healthcare).

The assembled *Hs* NOT module was obtained by co-expression of MBP-tagged NOT1 SHD (residues 1833–2361), MBP-tagged NOT2 (residues 350–540) and His_6-tagged NOT3 (residues 607–748). The cells were lysed in lysis buffer supplemented with DNaseI, lysozyme and protease inhibitors. The protein complex was purified over amylose resin and eluted with lysis buffer supplemented with 25 mM D-(+)-maltose and 20 mM imidazole. The NOT module was further purified via nickel affinity chromatography using a HiTrap IMAC column (GE Healthcare). The affinity tags were removed by overnight cleavage using HRV3C protease during dialysis in a buffer containing 50 mM Tris-HCl (pH 8.6), 200 mM NaCl, 10% glycerol and 2 mM DTT. The cleaved MBP tags were removed by binding to amylose resin. The remaining contaminants were removed by size-exclusion chromatography using a Superdex 200 column (GE Healthcare) in a buffer containing 10 mM Tris-HCl (pH 8.6), 200 mM NaCl, 10% glycerol and 2 mM DTT.

Crystallization

Initial screens were carried out using the sitting drop vapor diffusion method using 5 mg/ml of the *Hs* NOT module or a mixture containing the *Hs* NOT module (5 mg/ml) and a 1.5-fold molar excess of the *Dm* Nanos NBR peptide. Samples (200 nl) were preincubated for 1 hr in a buffer containing 10 mM Tris-HCl (pH 8.6), 200 mM NaCl, 10% glycerol and 2 mM DTT and were added to 200 nl of reservoir solution. Crystals appeared within three days in many different conditions containing polyethylene glycol (PEG). The best NOT module crystals were optimized to grow in 0.2 M sodium acetate, 0.1 M sodium citrate (pH 5.5) and 10% (w/v) PEG 4000. The best-diffracting crystals of the NOT module bound to the Nanos peptide were optimized to grow over a week in 100 mM MES (pH 6.0), 260 mM LiCl and 18.6% (w/v) PEG

6000. Crystals were cryoprotected using reservoir solution supplemented with 15% glycerol and flash-frozen in liquid nitrogen.

Data collection and structure determination

Diffraction data were recorded on a PILATUS 6M detector at the PXII beamline of the Swiss Light Source (SLS) at a temperature of 100 K. Data were processed using XDS and XSCALE (Kabsch, 2010). Initial phase information was obtained by molecular replacement with the structure of the *Hs* NOT module (PDB code 4C0D) as a search model using PHASER (McCoy *et al*, 2007) from the CCP4 package (Winn *et al*, 2011). The models were then improved by iterative cycles of refinement using PHENIX (Afonine *et al*, 2012) and BUSTER (Bricogne *et al*, 2011) and manual building in COOT (Emsley *et al*, 2010). Finally, the *Dm* Nanos NBR was built into the density and improved by several additional refinement cycles. Reported coordinate errors (Table 1) are from BUSTER and correspond to the diffraction-component precision index (Blow, 2002).

Anomalous difference Fourier map

Anomalous data were also recorded at the PXII beamline, at a wavelength of 0.979 Å and to a resolution of 3.9 Å. Data were processed and scaled using XDS and XSCALE, keeping Friedel mates apart to extract the anomalous difference for the calculation of the map coefficients. Phases were obtained from molecular replacement (PHASER) using the refined structure of the complex and searching for two copies, followed by one cycle of rigid body refinement in PHENIX.

Sequence searches and alignments

Nanos and NOT1–3 protein sequences were retrieved from TREEFAM (http://www.treefam.org) and aligned using the MAFFT webserver (http://mafft.cbrc.jp; L-INS-i preset) from within JALVIEW (http://www.jalview.org). Positional conservation and similarity scores were calculated using the SCORECONS webserver (http://www.ebi.ac.uk/thornton-srv/databases/cgi-bin/valdar/scorecons_server.pl) with default settings. Alignments were illustrated manually.

Appendix References

Afonine PV, Grosse-Kunstleve RW, Echols N, Headd JJ, Moriarty NW, Mustyakimov M, Terwilliger TC, Urzhumtsev A, Zwart PH, Adams PD (2012) Towards automated crystallographic structure refinement with phenix.refine. *Acta Crystallogr D Biol Crystallogr* 68: 352 – 367

Blow DM (2002) Rearrangement of Cruickshank's formulae for the diffraction-component precision index. *Acta Crystallogr D Bio Crystallogr* 58: 792 – 797

Bricogne G, Blanc E, Brandl M, Flensburg C, Keller P, Paciorek W, Roversi P, Sharff A, Smart O.S, Vonrhein C, Womack TO (2011) BUSTER. Cambridge, United Kingdom: Global Phasing Ltd.

Cheng Y, Patel DJ (2004). An efficient system for small protein expression and refolding. *Biochemical and Biophysical Research Communications* 317: 401 – 405

Diebold ML, Fribourg S, Koch M, Metzger T, Romier C (2011) Deciphering correct strategies for multiprotein complex assembly by co-expression: application to complexes as large as the histone octamer. *J Struct Biol* 175: 178 – 188

Emsley P, Lohkamp B, Scott WG, Cowtan K (2010) Features and development of Coot. *Acta Crystallogr D Biol Crystallogr* 66: 486 – 501

Haas G, Braun JE, Igreja C, Tritschler F, Nishihara T, Izaurralde E (2010) HPat provides a link between deadenylation and decapping in metazoa. *J Cell Biol* 189: 289 – 302

Jeske M, Meyer S, Temme C, Freudenreich D, Wahle E (2006) Rapid ATP-dependent deadenylation of nanos mRNA in a cell-free system from Drosophila embryos. *J Biol Chem* 281: 25124 – 25133

Kabsch W (2010) XDS. *Acta Crystallogr D Biol Crystallogr* D66: 125 – 132

McCoy AJ, Grosse-Kunstleve RW, Adams PD, Winn MD, Storoni LC, Read RJ (2007) Phaser crystallographic software. *J Appl Crystallogr* 40: 658 – 674

Tritschler F, Eulalio A, Helms S, Schmidt S, Coles M, Weichenrieder O, Izaurralde E, Truffault V (2008) Similar modes of interaction enable Trailer Hitch and EDC3 to associate with DCP1 and Me31B in distinct protein complexes. *Mol Cell Biol* 28: 6695 – 6708

Winn MD, Ballard CC, Cowtan KD, Dodson EJ, Emsley P, Evans PR, Keegan RM, Krissinel EB, Leslie AG, McCoy A, *et al.* (2011) Overview of the CCP4 suite and current developments. *Acta Crystallogr D Biol Crystallogr* 67: 235 – 242

Appendix Figure S1. Raisch et al.

NOT1

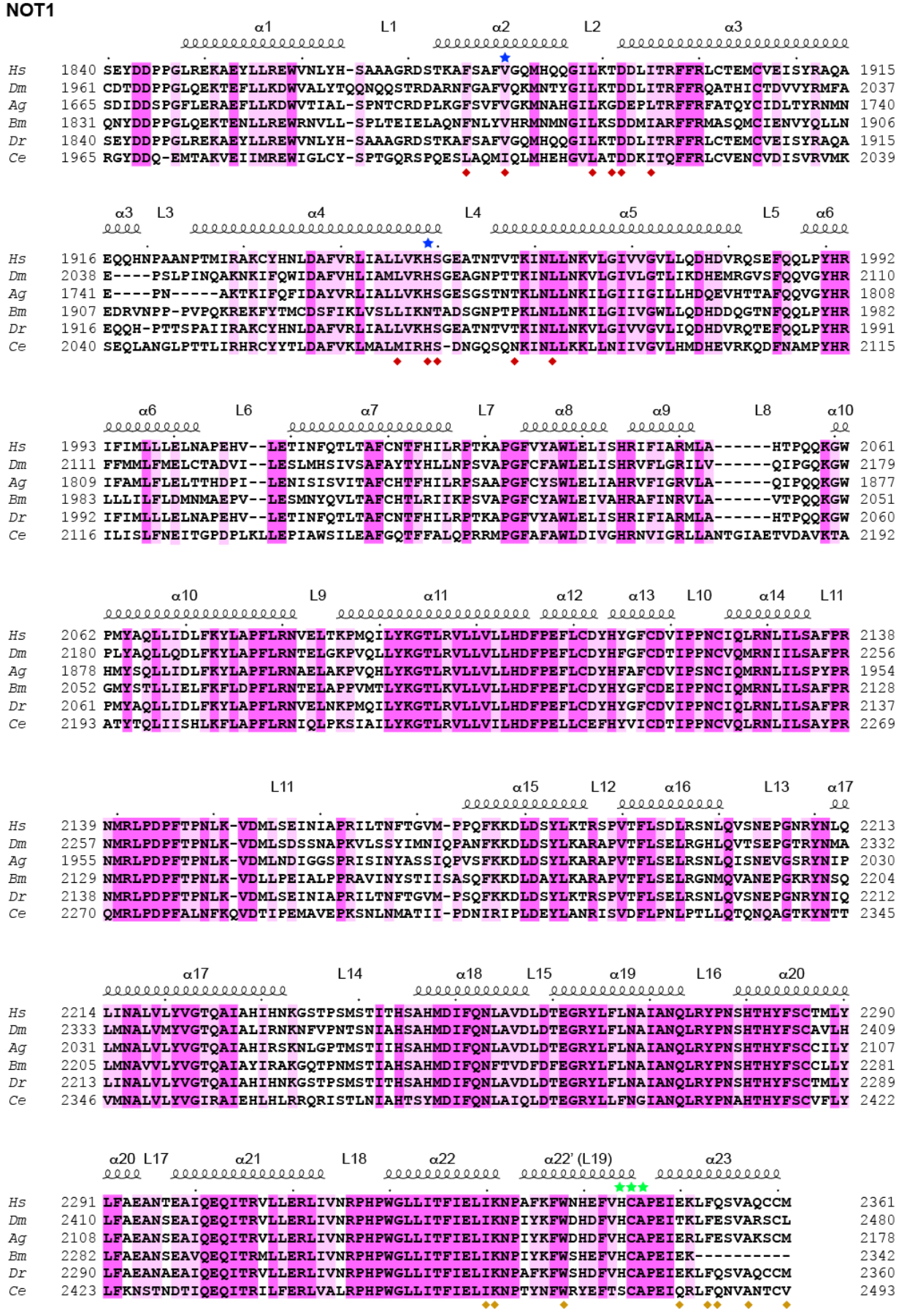

Appendix Figure S1. Sequence alignment of the NOT1 SHD.

The secondary structural elements as determined from the *Hs* NOT1 structure are shown above the alignment. The residues conserved in all of the aligned sequences are shown on a dark magenta background, and the residues with >70% similarity are shown on a light magenta background. The residues interacting with the *Dm* NBR and the human Nanos1 NIM peptide are indicated by red and orange diamonds, respectively. The residues mutated in this study are indicated by asterisks colored in blue (mutations that disrupt NBR binding) or in green (crystallization mutations). Loop L19 as observed in the previous structure of the NOT module (PDB entry 4C0D) folds as an α-helix (α22') in the present structures. The species abbreviations are as follows: *Hs* (*Homo sapiens*), *Dm* (*Drosophila melanogaster*), *Ag* (*Anopheles gambiae*), *Bm* (*Bombyx mori*), *Dr* (*Danio rerio*), and *Ce* (*Caenorhabditis elegans*).

Appendix Figure S2. Raisch et al

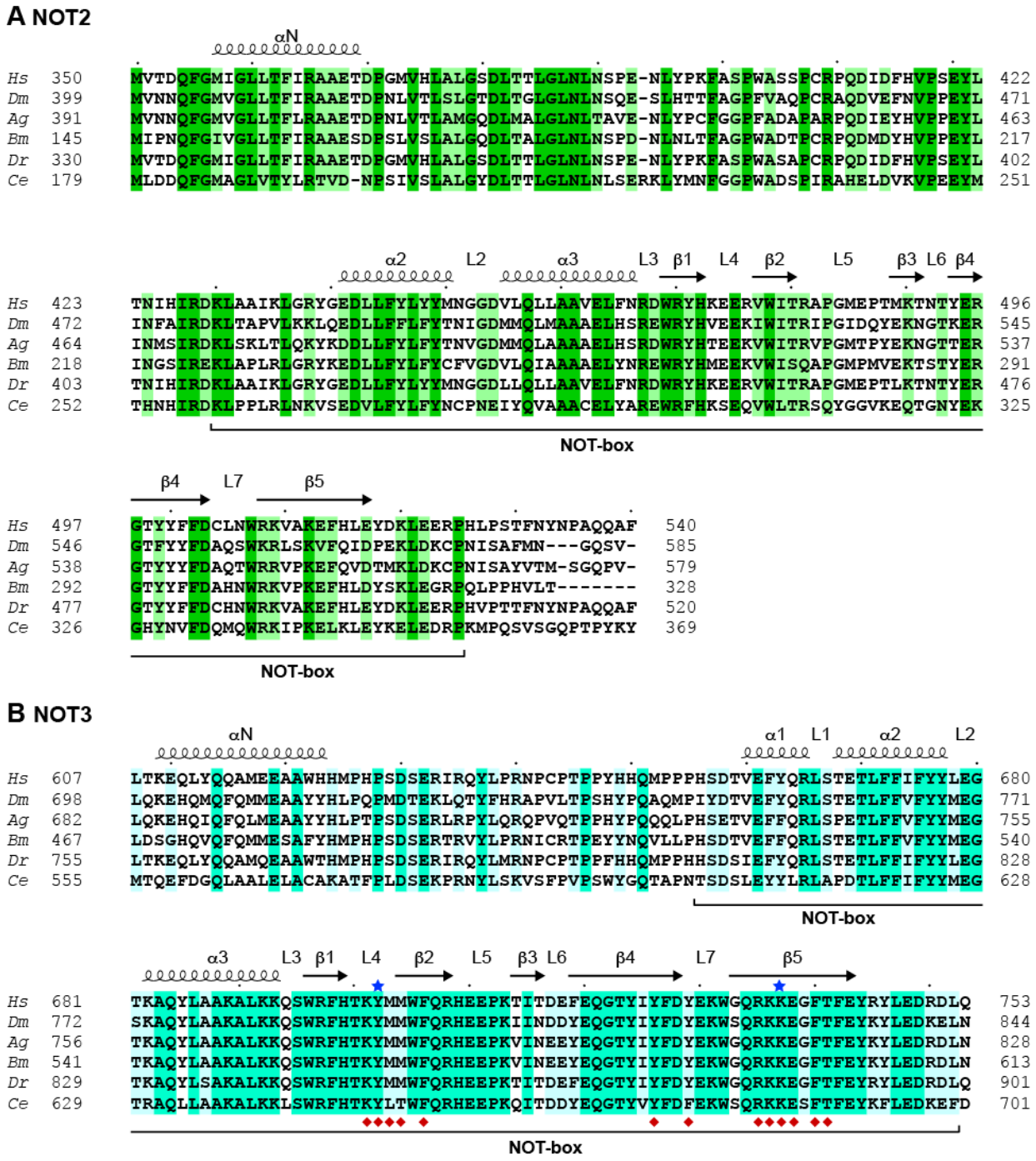

Appendix Figure S2. Sequence alignment of the NOT2 and NOT3 C-terminal fragments.

A,B The secondary structural elements as determined from the *Hs* NOT module structure are shown above the alignment. The residues conserved in all of the aligned sequences are shown with a dark green (NOT2) or cyan (NOT3) background, and the residues with >70% similarity are highlighted with a light green or cyan background. The NOT3 residues

interacting with the *Dm* NBR are indicated by red diamonds. The residues mutated in this study are indicated by blue asterisks. The species abbreviations are as described in Appendix Fig S1.

Appendix Table S1. Constructs used in this study.

***Dm* Nanos, isoform B** (Uniprot A0A0B4KGY5-1)		**Comment**
Full length	λN-HA-Nanos	
	GFP-Nanos	
ΔZnF	λN-HA-Nanos 1–296	
	GFP-Nanos 1–296	
ZnF	λN-HA-GST-Nanos 297–381	
	GFP-Nanos 297–381	
NED	GST-Nanos 50–236-GB1	
	λN-HA-GST-Nanos 50–236	
	GFP-Nanos 50–236	
Nanos-ΔNED	λN-HA-Nanos Δ50–236	
	GFP-Nanos Δ50–236	
NED ΔNBR	GST-Nanos 50–236-Δ116–163-GB1	
NBR	GST-Nanos 116-163	
	λN-HA-GST-Nanos 116–163	
NBR 3xMut	GST-Nanos 116–163 E151A,F152A,N155A	Mutation disrupts NOT3 binding
	λN-HA-GST-Nanos 116–163 E151A,F152A,N155A	Mutation disrupts NOT3 binding
NBR F152E	GST-Nanos 116–163 F152E	Mutation disrupts NOT3 binding
	λN-HA-GST-Nanos 116–163 F152E	Mutation disrupts NOT3 binding
NBR 2xMut	GST-Nanos 116–163 L127D,F130D	Mutation disrupts NOT1 binding
	λN-HA-GST-Nanos 116–163 L127D,F130D	Mutation disrupts NOT1 binding
NBR I123M	GST-Nanos 116–163, I123M	SeMet labeling
50–115	λN-HA-GST-Nanos 50–115	
164–236	λN-HA-GST-Nanos 164–236	
***Hs* Nanos2** (Uniprot P60321) **- *Dm* Nanos chimera**		
NIM-ZnF	λN-HA-GST-*Hs* Nanos2 NIM-*Dm* Nanos 297–381	
NIM*ZnF	λN-HA-GST-*Hs*Nanos2 NIM (F6A,W9E)-*Dm*Nanos 297–381	
***Hs* Nanos3** (Uniprot P60323)		
NIM	MBP-*Hs* Nanos3 4–20-Strep	
***Hs* NOT1** (CNOT1, Uniprot A5YKK6)		
MBP-NOT1-SHD	MBP-*Hs* NOT1 1833–2361	
MBP-NOT1-SHD EEE	MBP-*Hs* NOT1 1833–2361 H2344E,C2345E,A2346E	Crystallization mutant L19
MBP-NOT1-SHD V1880E	MBP-*Hs* NOT1 1833–2361 V1880E	Disrupts Nanos binding
MBP-NOT1-SHD H1949D	MBP-*Hs* NOT1 1833–2361 H1949D	Disrupts Nanos binding
***Hs* NOT2** (CNOT2, Uniprot Q9NZN8)		
NOT2-C	MBP-*Hs* NOT2 350–540	

***Hs* NOT3** (CNOT3, Uniprot O75175)		
NOT3-C	6xHis-*Hs* NOT3 607–748	
NOT3-C Y702A	6xHis-*Hs* NOT3 607–748 Y702A	Disrupts Nanos binding
***Dm* NOT1, isoform C** (Uniprot A8DY81)		
NOT1-C V2002E	λN-HA-NOT1 1710–2505 V2002E	Disrupts Nanos binding
NOT1-C H2067D	λN-HA-NOT1 1710–2505 H2067D	Disrupts Nanos binding
NOT1-C	λN-HA-NOT1 1710–2505	
NOT1-ΔC	λN-HA-NOT1 Δ1710–2505	
***Dm* NOT3** (Uniprot Q7K126)		
NOT3-N	λN-HA-NOT3 1–246	
NOT3-L	λN-HA-NOT3 239–681	
NOT3-C	λN-HA-NOT3 677–844	
***Dm* NOT2** (Uniprot Q94547)		
NOT2-N	λN-HA-NOT2 1–401	
NOT2-C	λN-HA-NOT2 402–585	
Dm hunchback (Flybase ID: FBgn0001180)		
F-Luc-*hb* 3'UTR	F-Luc-*hunchback* 3'UTR	
ΔBoxA	F-Luc-*hunchback*- 3'UTR Δ(2495–2499)nt Δ(2546–2550)nt	
ΔBoxB	F-Luc-*hunchback*- 3'UTR Δ(2505–2510)nt Δ(2556–2561)nt	

Appendix Table S2. Antibodies used in this study.

Antibody	**Source**	**Catalog Number**	**Dilution**	**Monoclonal/ Polyclonal**
Anti-HA-HRP (for western blots)	Roche	12 013 819 001	1:5,000	Monoclonal
Anti-HA (for immunoprecipitations)	Covance	MMS-101P		Mouse monoclonal
Anti-GFP (for western blots)	Roche	11 814 460 001	1:2,000	Mouse monoclonal
Anti-GFP (for immunoprecipitations)	In house	Tritschler *et al*, 2008		Rabbit polyclonal
Anti-mouse IgG-HRP	GE Healthcare	NA931V	1:10,000	Sheep polyclonal
Anti-rabbit IgG-HRP	GE Healthcare	NA934V	1:10,000	Donkey polyclonal
Anti-*Dm* NOT1	Kind gift from E. Wahle	Jeske *et al*, 2006	1:1,000	Rabbit polyclonal
Anti-*Dm* NOT2	Kind gift from E. Wahle	Jeske *et al,* 2006	1:3,000	Rabbit polyclonal
Anti-*Dm* NOT3	Kind gift from E. Wahle	Jeske *et al*, 2006	1:3,000	Rabbit polyclonal
Anti-tubulin	Sigma Aldrich	T6199	1:10,000	Mouse monoclonal